Journal of Ceramic Processing Research. Vol. 17, No. 8, pp. 894~898 (2016)

J O U R N A L O F
Ceramic Processing Research

High density plasma etching of YSZ thin film in halogen-based inductively coupled plasmas

Byoung Su Choi[a], Jong Cheon Park[a], Jun Won Seo[b], Su Chak Ryu[b], Hee Soo Lee[c], Jeong Ho Ryu[d] and Hyun Cho[b,*]

[a]*Department of Nano Fusion Technology, Pusan National University, Gyeongnam 50463, Korea*
[b]*Department of Nanomechatronics Engineering, Pusan National University, Busan 46241, Korea*
[c]*School of Materials Science & Engineering, Pusan National University, Busan 46241, Korea*
[d]*Department of Materials Science and Engineering, Korea National University of Transportation, Chungbuk 27469, Korea*

Yttria-stabilized zirconia (YSZ) has a good potential as a gate dielectric in various metal-oxide-semiconductor field effect transistor (MOSFET) devices for displays and a precise and anisotropic plasma etching is required for the integration of the YSZ gate structure. High density plasma etching of YSZ thin film was performed in halogen-based inductively coupled plasmas (ICPs) and the effect of process variables such as plasma composition, ICP source power and rf chuck power on the YSZ etch characteristics was examined. Higher YSZ etch rates were obtained in chlorine-based ($10BCl_3/5Ar$ and $10Cl_2/5Ar$) ICP discharges because of the higher volatilities of metal chloride etch products. Maximum etch rates of 1042.5 Å/min and 796 Å/min were obtained in $10BCl_3/5Ar$ and $10CF_4/5Ar$ ICP discharges, respectively. $10CF_4/5Ar$ discharges were found to provide a very smooth surface morphology while a significant surface roughening has occurred after etching at high rf chuck power conditions in $10BCl_3/5Ar$ discharges. The YSZ surfaces etched in $10BCl_3/5Ar$ and $10CF_4/5Ar$ maintained the stoichiometry and highly anisotropic features were transferred into YSZ by $10CF_4/5Ar$ ICP etching.

Key words: YSZ thin film, High density plasma etching, Halogen-based inductively coupled plasmas, Etch rate, Etch selectivity, Anisotropy.

Introduction

Recently, as gate dielectric thickness in metal-oxide-semiconductor field effect transistors (MOSFETs) have been scaled down, it has been recognized that the conventional SiO_2 and SiON gate dielectrics cannot sustain the gate capacitance without increasing the leakage current. When the thickness of SiO_2 gate is reduced to below ~2 nm, the leakage current rises to 1-10 $A \cdot cm^{-2}$ due to the exponential increase in tunneling current, and this leads to a significant power dissipation [1-3]. On the contrary, high dielectric constant materials ($k > 20$) can provide the reduced leakage current characteristics while maintaining the same gate capacitance, and they are expected to be able to extend scaling to an equivalent oxide thickness in the sub-1 nm regime [4-6]. A number of high-k materials such as Al_2O_3, Ta_2O_5, TiO_2, $ZrSiO_4$, $Zr_{1-x}Al_xO_y$, HfO_2, Y_2O_3, ZrO_2, and yttria-stabilized zirconia (YSZ) were studied to replace SiO_2 and SiON [7-13]. These high-k materials should also meet the requirements such as thermodynamic stability with semiconductor, low interface state densities and availability of conformal deposition over morphological features, etc. to be used as gate dielectrics for advanced MOSFET devices. YSZ is one of the most attractive candidates due to its high-k value (~25), good thermal stability at the interface with Si and high diffusion resistance to dopants [14-16]. Moreover, it has been recently reported that YSZ has a good potential as a gate dielectric material in amorphous $InGaZnO_4$ (a-IGZO) thin film transistors (TFTs) for transparent displays and flexible displays since YSZ offers a sufficiently large conduction band offset for carrier confinement in heterojunctions with a-IGZO [17].

In the integration of YSZ thin films on the MOSFET devices, a precise pattern transfer is very important to reduce contact resistance and obtain a reliable device performance. High density plasma etching would be the best choice to satisfy the requirements such as practical and controllable etch rate, low ion-induced damage, residue-free, anisotropic feature formation and smooth surface morphology. Up to now, very little work has been reported on the plasma etching of YSZ film [18]. In this work, we report on the high density plasma etching of sputter-deposited YSZ films in chlorine- and fluorine-based (BCl_3/Ar, Cl_2/Ar, CF_4/Ar and SF_6/Ar) inductively coupled plasmas (ICPs). The effect of plasma composition, ion flux and ion energy on the YSZ etch characteristics was studied.

Experimental

YSZ films were deposited on the Φ4" Si substrates

*Corresponding author:
Tel : +82-51-510-6113
Fax: +82-51-514-2358
E-mail: hyuncho@pusan.ac.kr

by rf magnetron sputtering with a commercial Φ3", 8 mol% yttria-stabilized zirconia target. Typical film thicknesses were ~5000 Å. As-deposited YSZ films were patterned with either AZ 5214 photoresist or ~500 Å thick nickel layer. High density plasma etching was performed in a planar inductively coupled plasma source operating at 13.56 MHz and power up to 1000 W, and the samples were thermally bonded to a Si carrier wafer that was mechanically clamped to a He backside-cooled, rf-powered (13.56 MHz, up to 450 W) chuck. Chlorine- (BCl_3 and Cl_2) and fluorine- (CF_4 and SF_6) based inductively coupled plasmas were employed to etch YSZ films. Ar gas was used as an additive gas and process pressure was varied from 2-20 mTorr, with a gas load of 15 standard cubic centimeters per minute (sccm). After removal of the mask materials, etch rates were measured by stylus profilometry. The surface morphology was characterized by tapping mode atomic force microscopy (AFM) and the anisotropy of etched features was examined by field-emission scanning electron microscopy (FE-SEM). The effect of plasma etching on the surface stoichiometry was examined by x-ray photoelectron spectroscopy (XPS).

Results and Discussion

Fig. 1 shows the effect of ICP source power on the YSZ etch rate in chlorine- and fluorine-based ICP discharges at fixed plasma composition, rf chuck power and pressure. Chlorine-based ICP discharges produce higher etch rates than fluorine-based discharges. This can be readily explained by comparing the volatility of metal chloride and metal fluoride etch products. The metal chloride etch products (presumably YCl_3; b.p. 1507 °C and $ZrCl_4$; b.p. 331 °C) have higher volatilities than the metal fluoride etch products (presumably YF_3; b.p. 2230 °C, and ZrF_4; b.p. 913 °C), which leads to the higher YSZ etch rates with chlorine-based ICP plasmas. In $10BCl_3/5Ar$ and $10CF_4/5Ar$ ICP discharges, the YSZ etch rate initially increases as source power increases due to the increased ion flux and the atomic chlorine or fluorine density, and after reaching the maximum etch rates (1042.5 Å/min for $10BCl_3/5Ar$ and 796 Å/min for $10CF_4/5Ar$), it decreases beyond 500 W source power. This is attributed to the trade-off between the increased ion flux and the decreased ion energy. The formation of etch products by the chemical reaction between the YSZ surface atoms and the adsorbed chlorine or fluorine neutrals should be balanced with ion-assisted desorption. At the source powers higher than 500 W, the ion flux keeps increasing, but the average ion energy in the plasma falls down below that needed to efficiently remove metal chloride or metal fluoride etch products from the surface. Therefore, the etching would be limited by ion-assisted desorption.

The influence of rf chuck power on the YSZ etch rate is presented in Fig. 2 for chlorine-and fluorine-based ICP discharges at a fixed source power (750 W) and pressure (2 mTorr). For both chlorine- and fluorine-based discharges, the YSZ etch rate increases continuously as rf chuck power increases, which indicates the presence of the physical component of the etching. In plasma-based dry etching, the energy of incident ions is directly controlled by rf chuck power. The average energy of Ar^+

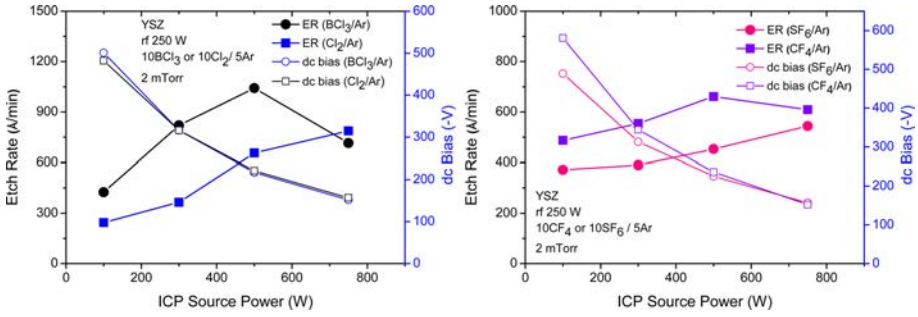

Fig. 1. YSZ etch rates as a function of ICP source power in chlorine- and fluorine-based ICP discharges (250 W rf chuck power, 2 mTorr pressure).

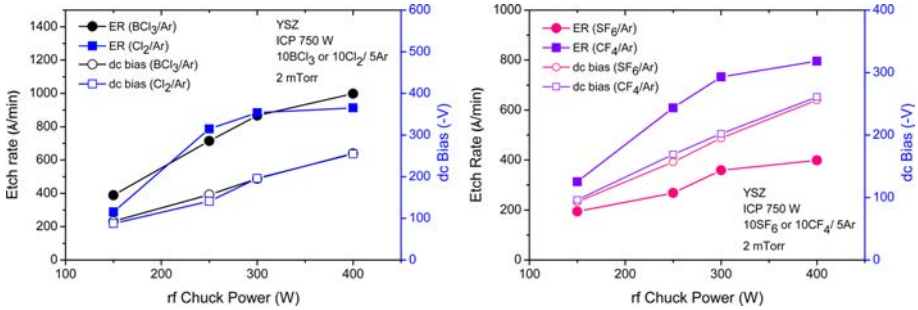

Fig. 2. YSZ etch rates as a function of rf chuck power in chlorine- and fluorine-based ICP discharges (750 W source power, 2 mTorr pressure).

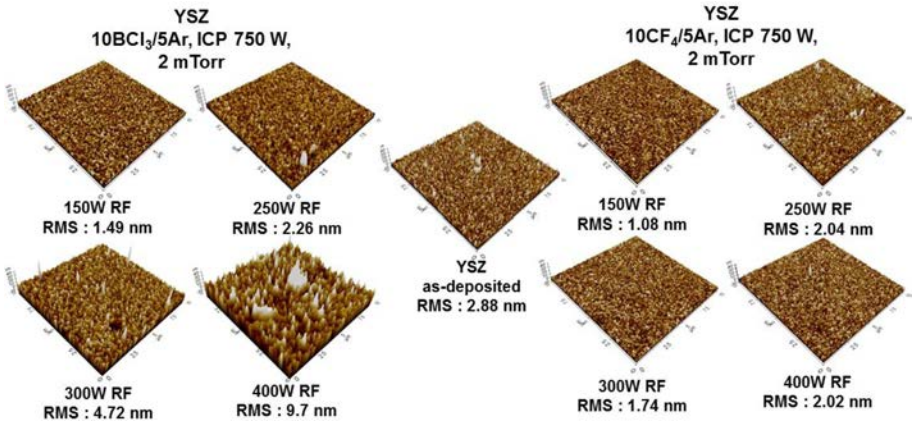

Fig. 3. AFM surface scan imges of YSZ films etched in $10BCl_3/5Ar$ and $10CF_4/5Ar$ ICP discharges (750 W source power, 2 mTorr pressure).

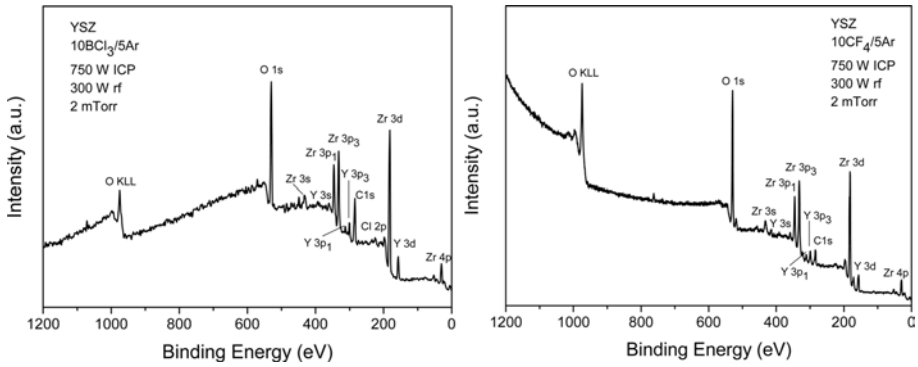

Fig. 4. XPS core level spectra of YSZ films etched in in $10BCl_3/5Ar$ and $10CF_4/5Ar$ ICP discharges (750 W source power, 300 W rf chuck power, 2 mTorr pressure).

ions that bombard the YSZ surface increase as rf chuck power increases, which enhances the ion-assisted desorption of the metal chloride or metal fluoride etch product from the surface. Therefore the rate-limiting step under these conditions would be the formations of the metal chloride or metal fluoride etch products by the chemical reaction between the YSZ surface atoms and the adsorbed reactive species.

Fig. 3 shows the AFM scan images of the YSZ surfaces etched in $10BCl_3/5Ar$ and $10CF_4/5Ar$ ICP discharges as a function of rf chuck power at a fixed source power (750 W) and pressure (2 mTorr). In each sample, the etch depth was maintained at ~2500 Å and root-mean-square (RMS) roughness of the unetched YSZ control sample was ~ 2.88 nm. The YSZ samples etched in $10CF_4/5Ar$ ICP discharges show better surface morphology than the unetched control sample under the conditions examined due to the ion-enhanced removal of metal fluoride etch products or sharp features from the surface. However, a severe degradation in surface morphology with the normalized roughness in the range of 1.64-3.37 compared to the unetched surface, most likely due to the inhomogeneous sputtering of surface atoms by the ion bombardments, has occurred after etching at high rf chuck power conditions in $10BCl_3/5Ar$ discharges. This result suggests that dry etching of YSZ films in CF_4/Ar ICP discharges would be a reasonable choice if a smooth surface finish is needed although they produce lower etch rates than chlorine-based ICP discharges.

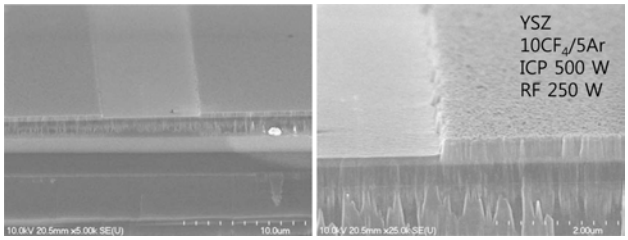

Fig. 5. SEM micrographs of features etched into YSZ using $10CF_4/5Ar$ ICP discharges (500 W source power, 250 W rf chuck power, 2 mTorr pressure).

XPS surface surveys of YSZ films etched in $10BCl_3/5Ar$ (left) and $10CF_4/5Ar$ (right) ICP discharges at 750 W source power, 300 W rf chuck power and 2 mTorr pressure are shown in Fig. 4. By comparing peak positions and relative intensities of the metal core levels with those of the unetched YSZ control sample, it was found that the YSZ samples etched in both of $10BCl_3/5Ar$ and $10CF_4/5Ar$ ICP discharges retained the stoichiometry which is very similar to that of the unetched YSZ surface. Please note that a signal of chlorine residue at the binding energy of 200-220 eV appeared on the $10BCl_3/5Ar$-etched YSZ surface and

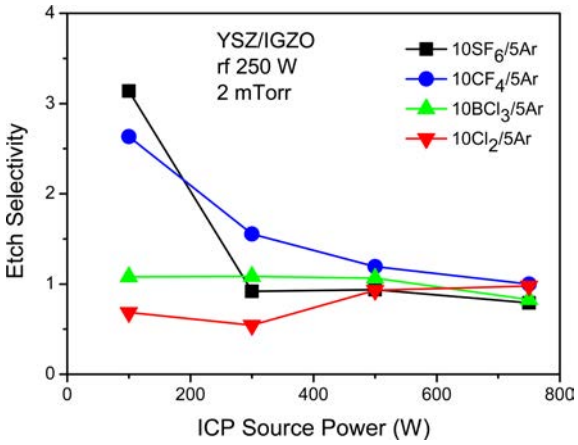

Fig. 6. Etch selectivity for YSZ over IGZO as a function of ICP source power (250 W rf chuck power, 2 mTorr pressure).

this needs to be removed by a post-etch cleaning for preventing the corrosion of metallic gate electrode layer [19].

Fig. 5 shows FE-SEM micrographs of features etched into YSZ films using $10CF_4/5Ar$ ICP discharges with a 500 W source power, 250 W rf chuck power, and 2 mTorr pressure. Please note that the Ni mask layer is still in place and the etch depth was maintained at ~ 2000 Å. As shown in Fig. 3, the etched YSZ surface shows a smooth surface morphology and a highly anisotropic pattern transfer with a vertical sidewall profile was performed with $10CF_4/5Ar$ discharges.

In the process for fabricating the YSZ gate dielectric on IGZO MOSFET devices, it is necessary to remove the YSZ layer selectively from an YSZ/IGZO multilayer structure and vice versa. Fig. 6 presents the etch selectivity for YSZ over IGZO as a function of source power in chlorine- and fluorine-based ICP discharges at a fixed plasma composition, rf chuck power (250 W) and pressure (2 mTorr). In fluorine-based ICP discharges, maximum etch selectivities of ~ 3.1 : 1 ($10SF_6/5Ar$) and ~ 2.6 : 1 ($10CF_4/5Ar$) are obtained at a low source power (100 W) and then the etch selectivity continuously decreases as source power increases further since, at source powers beyond 100 W, the YSZ etch rate shows a source power dependence (see Fig. 1) similar to that of the IGZO etch rate that we have previously reported elsewhere [20]. $10Cl_2/5Ar$ ICP discharges produce the etch selectivities ~0.6 at relatively low source powers (100 and 300 W) while the etch selectivities close to unity are obtained for $10BCl_3/5Ar$ discharges under the conditions examined. The IGZO TFTs with bottom-gate structure have been recently reported to present better performance than those with top-gate structure [21, 22], and $10Cl_2/5Ar$ ICP discharges under low source power conditions could be useful for fabricating the IGZO TFTs with the YSZ bottom-gate.

Conclusions

Parametric study of high density plasma etching of YSZ film was performed in chlorine- and fluorine-based (BCl_3/Ar, Cl_2/Ar, CF_4/Ar and SF_6/Ar) inductively coupled plasmas. 10 $BCl_3/5Ar$ and $10Cl_2/5Ar$ ICP discharges produced higher YSZ etch rates than fluorine-based discharges under most of the conditions examined due to the higher volatilities of metal chloride etch products compared to those of metal fluoride etch products. Maximum etch rates of 1042.5 Å/min and 796 Å/min were obtained in $10BCl_3/5Ar$ and $10CF_4/5Ar$ ICP discharges, respectively. For $10BCl_3/5Ar$ and $10CF_4/5Ar$ ICP discharges, the YSZ etch rate initially increased as source power increased, and then decreased at source power beyond 500 W due to the imbalance between the etch products formation and subsequent ion-assisted desorption while it showed a strong dependence on the rf chuck power. Surface stoichiometry of the YSZ films was found not to be significantly affected by $10BCl_3/5Ar$ and $10CF_4/5Ar$ ICP etching and the YSZ samples etched in $10CF_4/5Ar$ ICP discharges showed better surface morphology than the unetched control sample. Maximum etch selectivities of ~ 3.1 : 1 and ~2.6 : 1 for YSZ over IGZO were obtained at a low source power condition (100 W) in $10SF_6/5Ar$ and $10CF_4/5Ar$ ICP discharges, respectively.

References

1. S.J. Wang, C.K. Ong, S.Y. Xu, P. Chen, W.C. Tjiu, ACH. Huan, W.J. Yoo, J.S. Lim, W. Feng, and W.K. Choi, Semicond. Sci. Technol. 16 (2001) L13-L16.
2. S.H. Jeong, I.S. Bae, Y.S. Shin, S.-B. Lee, H.-T. Kwak, and J.-H. Boo, Thin Solid Films 475 (2005) 354-358.
3. D.A. Buchanan and S.H. Lo, Microelectron. Eng. 36 (1997) 13-20.
4. Z.J. Luo, X. Guo, T.P. Ma, and T. Tamagawa, Appl. Phys. Lett. 79 (2001) 2803-2804.
5. D. Han, J. Kang, C. Lin, and R. Han, Chin. Phys. 12 (2003) 325-327.
6. G.D. Wilk, R.M. Wallace, and J.M. Anthony, J. Appl. Phys. 89 (2001) 5243-5275.
7. D. Park, Y.C. King, Q. Lu, T.J. King, C. Hu, A. Kalnitsky, S.P. Tay, and C.C. Cheng, IEEE Electron. Dev. Lett. 19 (1998) 441-443.
8. G.B. Alers, D.J. Weider, Y. Chabal, H.C. Lu, E.P. Guser, E. Garfunkel, T. Gusrafson, and R.S. Urdahl, Appl. Phys. Lett. 73 (1998) 1517-1519.
9. S.H. Campbell, D.C. Gilmer, X. Wang, M. Hsieh, H.S. Kim, W.L. Gladfeter and J. Yan, IEEE Trans. Electron. Dev. 44 (1997) 104-109.
10. H.S. Kim, S.A. Campbell, and D.C. Gilmer, IEEE Electron. Dev. Lett. 18 (1997) 465-.
11. G.D. Wilk and R.M. Wallace, Appl. Phys. Lett. 76 (2000) 112-114.
12. Y. Ma, Y. Ohno, L. Stecher, D.R. Evans, S.T. Hsu, Proc. Tech. Dig. Int. Electron Devices Meet. 149 (1999).
13. J. Zhu and Z.G. Liu, Mater. Lett. 57 (2003) 4297-4301.
14. A.P. Caricato, A. Di Cristoforo, M. Fernandez, G. Leggieri,

A. Luches, G. Majni, M. Martino, and P. Mengucci, Appl. Surf. Sci. 208-209 (2003) 615-619.
15. M. Hartmanova, M. Jergel, V/ Navratil, K. Navratil, K. Gmucova, F.C. Gandarilla, J. Zemek, S. Chromik, and F. Kundracik, Acta Physica Slovaca 55 (2005) 247-259.
16. T. Ngai, W.J. Qi, R. Sharma, J. Fretwell, and X. Chen, Appl. Phys. Lett. 76 (2000) 502-504.
17. J.K. Kim, K.-W. Kim, E.A. Douglas, B.P. Gila, V. Craciun, E.S. Lambers, D.P. Norton, F. Ren, S.J. Pearton, and H. Cho, J. Nanosci. Nanotechnol. 14 (2014) 3925-3927.
18. M.S. Kiruba, R.LL. Rajeswara, and J. Nagaraju, J. Vac. Sci. Technol. B 33 (2015) 022003 (022003-1~022003-8).
19. K.B. Jung, H. Cho, K.P. Lee, J. Marburger, F. Sharifi, R.K. Singh, D. Kumar, K.H. Dahmen, and S.J. Pearton, J. Vac. Sci. Technol. B 17 (1999) 3186-3189.
20. J.C. Park, O.G. Jeong, J.K. Kim, Y.H. Yun, S.J. Pearton, and H. Cho, Thin Solid Films 546 (2013) 136-140.
21. K. Hosino, D. Hong, H.Q. Chiang, and J.F. Wager, IEEE Trans. Electron Devices 56 (2009) 1365-1370.
22. J.H. Na, M. Kitamura, and Y. Arakawa, Appl. Phys. Lett. 93 (2008) 063501 (063501-1~063501-3).